NANO LETTERS
2002
Vol. 2, No. 7
703−708

Synthesis of Ultralong and High Percentage of Semiconducting Single-walled Carbon Nanotubes

Woong Kim, Hee Cheul Choi, Moonsub Shim, Yiming Li, Dunwei Wang, and Hongjie Dai*

Department of Chemistry, Stanford University, Stanford, California 94305

Received May 2, 2002; Revised Manuscript Received May 15, 2002

ABSTRACT

Two main results are reported here for single-walled carbon nanotubes (SWNTs) synthesized from well-controlled isolated catalytic Fe_2O_3 nanoparticles. The first is patterned growth of ultralong SWNTs (lengths up to 0.6 millimeters) by using a mixed methane and ethylene carbon source in chemical vapor deposition (CVD). Interesting loop and closed ring structures similar to those of fullerene "crop circles" are observed on these as-grown ultralong tubes. Second, surveying the electronic properties of individual SWNTs by transport measurements reveals that approximately 70% of individual SWNTs grown from isolated nanoparticles are semiconductors exhibiting field effect transistor (FET) characteristics. The distribution of CVD-grown SWNT chirality is elucidated for the first time, and implications to array-based nanotube electronics and sensors are discussed.

The synthesis of single-walled carbon nanotubes has recently been carried out with isolated discrete catalytic nanoparticles carefully derived by wet chemical routes, aimed at controlling the structure (e.g., diameter) of these novel nanowires.[1−3] The highly sensitive structure−property relations[4] in nanotubes require control of nanotube diameter and chirality in order to predict the growth of metallic or semiconducting molecular wires. Although not yet at hand, a path to such control could be via the control of catalytic "seeds" and understanding how seed particles determine the nanotube diameter and chirality.[5,6] Progress has indeed been made along this line. With powder-based supported catalyst, SWNTs synthesized by CVD have a wide diameter distribution of 1−5 nm. Using isolated nanoparticles synthesized in apoferritin as catalyst, one can narrow down the diameters of CVD-grown nanotubes to 1−3 nm.[1] Further narrowing of the diameters of CVD tubes to 1−2 nm is achieved recently using nanoparticles derived on dendrimer templates.[7]

This letter follows up on the synthesis and properties of SWNTs grown from ferritin. New structural data of nanotubes is obtained, and the electronic properties of isolated SWNTs are surveyed statistically. The results include the growth of SWNTs into macroscopic lengths up to 0.6 mm, the longest reported for isolated single-walled tubes. The nanotubes exhibit interesting loop and ring morphologies in their as-grown forms. Multiprobe transport study reveals no apparent changes in chirality along the lengths of these long tubes. Measurements over large numbers of individual SWNTs reveal that about 70% of the nanotubes are semiconductors and others being small band gap semiconductors and metals. The results combined with structure−property analysis suggest that SWNTs grown from our current method in fact do not favor any tube chirality. Nevertheless, the high yield and "natural abundance" of semiconducting nanotubes in the synthesis is welcome and can be exploited in building large arrays of nanotube transistors and sensors.

The synthesis of Fe_2O_3 nanoparticles with ferritin has been described previously.[1] We deposit ferritin from a 1.6 μM water solution into an array of square wells[8,9] of polymethylmathacrylate (PMMA) patterned photolithographically on a SiO_2 substrate by incubating the substrate in the ferritin solution for 2 h. Liftoff of PMMA followed by calcination[1] in air results in a submonolayer of catalytic Fe_2O_3 nanoparticles confined in square regions (side length 0.1−3 μm) on SiO_2. Nanotube growth on the substrate takes place in a 1 in. tube-furnace at 900 °C for 10 min under combined flows of 1000 sccm (standard cubic centimeter per minute) of CH_4 (99.999%, gas correction factor 0.72), 500 sccm of H_2 (gas correction factor 1.01), and 20 sccm of C_2H_4 (gas correction factor 0.60). Note that the combination of gases here differs slightly from our previous recipe for SWNT growth.[1,8,9]

Atomic force microscopy (AFM) imaging reveals that SWNTs are reliably grown and emanating from the patterned catalyst sites. The average number of nanotubes grown from each square decorated by Fe_2O_3 nanoparticles is 1−5. Statistics show about 30% of the isolated nanotubes grown on a substrate are very long, with lengths ≥ 100 μm, and

* Corresponding author. Phone: (650) 723-4518. Fax: (650) 725-0259. E-mail: hdai1@stanford.edu.

10.1021/nl025602q CCC: $22.00
Published on Web 06/01/2002

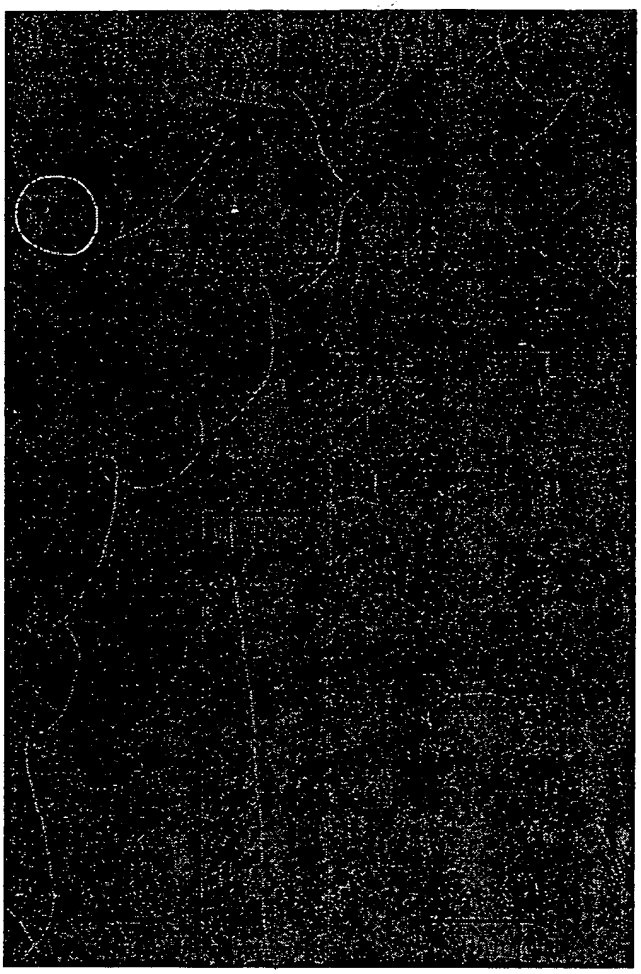

Figure 1. Very long as-grown single-walled carbon nanotubes. (a) A mosaic of AFM images for a 320 μm long nanotube (diameter ~2 nm). The nanotube is grown from a catalyst particle in a patterned region circled at the bottom of the figure. See text for the formation of loop structures. (b) AFM image of a 40 μm long straight nanotube grown from a patterned catalyst site (circled at the bottom). (c) AFM image of a 110 μm long nanotube. (d) AFM image showing a closed ring near the extended end of a long tube.

the longest SWNT observed is ~600 μm. Figure 1a is a mosaic of AFM images showing a 320 μm long SWNT (diameter = 2 nm) grown from a catalyst square (circled region at the bottom of Figure 1a). The nanotube exhibits 14 oval-shaped loops (diameters ~ 2 μm) along its length (the last tube section is not shown, limited by figure size). While nanotubes tens of microns long are typically relatively straight (Figure 1b), tubes that are hundreds of microns long tend to show loop structures along their length. A second example is shown in Figure 1c in which a 110 μm long nanotube contains 7 loops.

Completely closed ring structures are observed on about 5−10% of the very long nanotubes. Shown in Figure 1d is the end section of a 160 μm long nanotube containing such a ring with a topographic height along its circumference ~10 nm (high brightness) compared to the 2.2 nm height along the rest of the tube. It can be gleaned that the ring is formed by the nanotube looping around for about 10 turns into a circular self-bundle. At the end of the nanotube, there is a 380 nm long segment not included into the bundle structure, as it branches off from the ring (Figure 1d). The loop and closed ring structures here are observed with as-grown SWNTs, different from those observed after post-growth treatment in liquids.[10−12]

The loops and rings are most likely formed in free space during SWNTs growth before they land on the substrate. As a SWNT grows out from the substrate into space, with a high aspect ratio of $>10^5$, it can loop around to cross itself to form van der Waals (vdW) point contacts, or loop around multiple times to make vdW line contacts with itself to form a ring. The vdW contacting and thermal energies overcome mechanical bending energy of the nanotube, leading to stable formation of loop and ring structures. The persistence length of a SWNT is ~0.8 μm,[12] and thermal energy at the high growth temperature is sufficient to cause nanotube looping with a radius on the order of ~1 μm. There is a possibility that the loop structures are formed when a loop-free and relatively straight tube in free space contacts a substrate. This explanation, however, is not plausible for the formation of closed rings with multiple loops.

The growth condition for isolated long SWNTs is robust and reproducible. Methane, hydrogen, and ethylene flows are balanced to enable continuous carbon feeding and nanotube growth while preventing catalyst poisoning by amorphous carbon deposition. We have not been able to grow similar yield of long tubes with methane or ethylene alone, suggesting that the combination of methane and ethylene is important to provide efficient carbon feedstock needed for nanotube growth. On the other hand, balancing with hydrogen[13] prevents excess carbon deposition from poisoning the catalyst and sustains nanotube growth over an extended period of time. Long SWNTs have been synthesized previously by using methane and a conditioning approach that generates higher hydrocarbons in situ,[14] which motivates the current growth condition with the intentional addition of ethylene. The results here provide important information about the growth rate of SWNTs in CVD. A SWNT can grow at >60 μm/min, and a reaction time of 10 s can already produce nanotubes with micron scale length in CVD. Typical transmission electron microscopy (TEM) data are shown in Figure 2 to confirm[1,2] that the nanotubes are indeed single-walled.

Next, we focus on elucidating the physical properties of SWNTs thus produced. Device fabrication involves microfabrication with the substrates containing SWNTs emanating from well-defined surface sites.[9] Titanium is used as electrodes for contacting nanotubes, and the Si substrate under the SiO_2 surface layer is used as a gate. We have carried out multiprobe (Figure 3a,b) electrical measurements on a total of 9 SWNTs with lengths >100 μm. Eight out of the nine tubes are found to be semiconductors exhibiting FET characteristics. Figure 3c,d shows the current vs gate ($I-V_g$) curves for a 700 nm long straight and a 21 μm long loop segments respectively on a long tube. Both segments exhibit hole-carrier depletion by positive gate, typical of p-type semiconductors.[15,16] The transconductance dI/dV_g for the short and straight segments is 1.7×10^{-7} A/V with a resistance of 95 kΩ at $V_g = -10$ V. Transconductance for

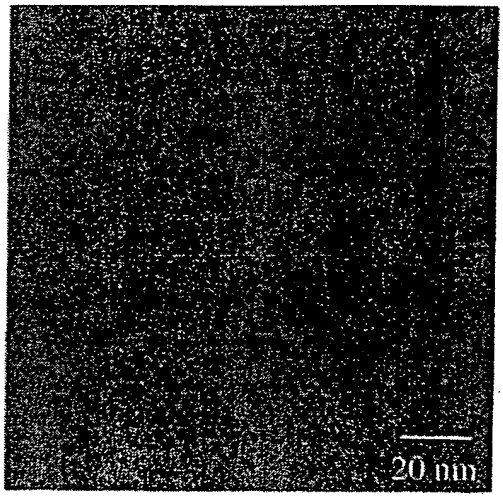

Figure 2. TEM image of a SWNT (diameter ~3 nm) grown from catalytic nanoparticles derived from ferritin.

the long loop segment is much lower, $\sim 8.6 \times 10^{-9}$ A/V, and the resistance is 2.7 MΩ at $V_g = -10$ V. These results combined with similar data acquired with other tubes suggest that the semiconducting nature of the nanotubes is retained along their lengths, indicating the absence of topological defects that cause apparent chirality change along the tube. Detailed length dependent transport properties and the effects of mechanical bending in the loop structures are being investigated currently.

To investigate the electronic nature of the SWNTs synthesized, we have measured 40 individual nanotubes with diameters ranging from 1 to 3 nm. It is known that SWNTs can be categorized into three types (Figure 4), truly metallic armchair SWNTs with (n,n) indices, semiconducting (m,n) SWNTs (S−SWNTs) with $m-n \neq 3\times integer$, and small band-gap semiconducting single-walled nanotubes (SGS−SWNTs) with $m-n = 3\times integer$ and $m \neq n$.[17−21] Considering all possible chiralities for SWNTs with diameters in the range of 1 to 3 nm, one identifies a total of 403 different nanotubes, as summarized in Table 1. If there is no preference in chirality, 3.5%, 31%, and 65.5% of the 403 nanotubes are metals, small gap tubes, and semiconductors, respectively.

Out of the 40 individual isolated SWNTs (Table 2), electrical transport measurements reveal that 25 (62.5%) are

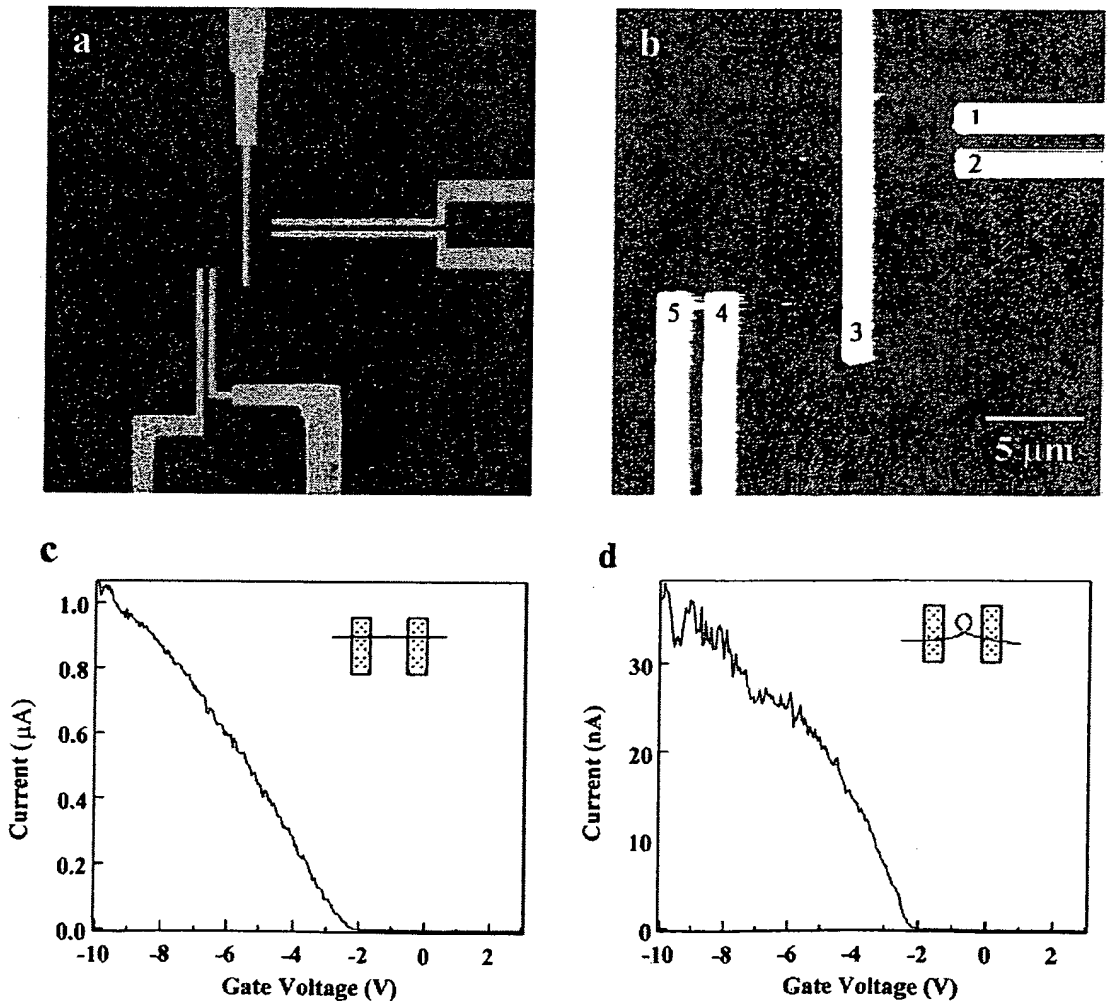

Figure 3. Multiprobe electrical measurements of long tubes. (a) Optical image of a device with five metal electrodes designed to contact a long SWNT. (b) AFM image showing the electrodes contacting the long nanotube with straight sections (between electrode pair: 1−2 and 5−4) and loop sections (between 2−3 and 3−4). (c) $I-V_g$ curve for a 700 nm long straight segment between 1 and 2 electrodes. (d) $I-V_g$ curve for a 21 μm long loop section between electrodes 2−3. Bias voltage = 100 mV.

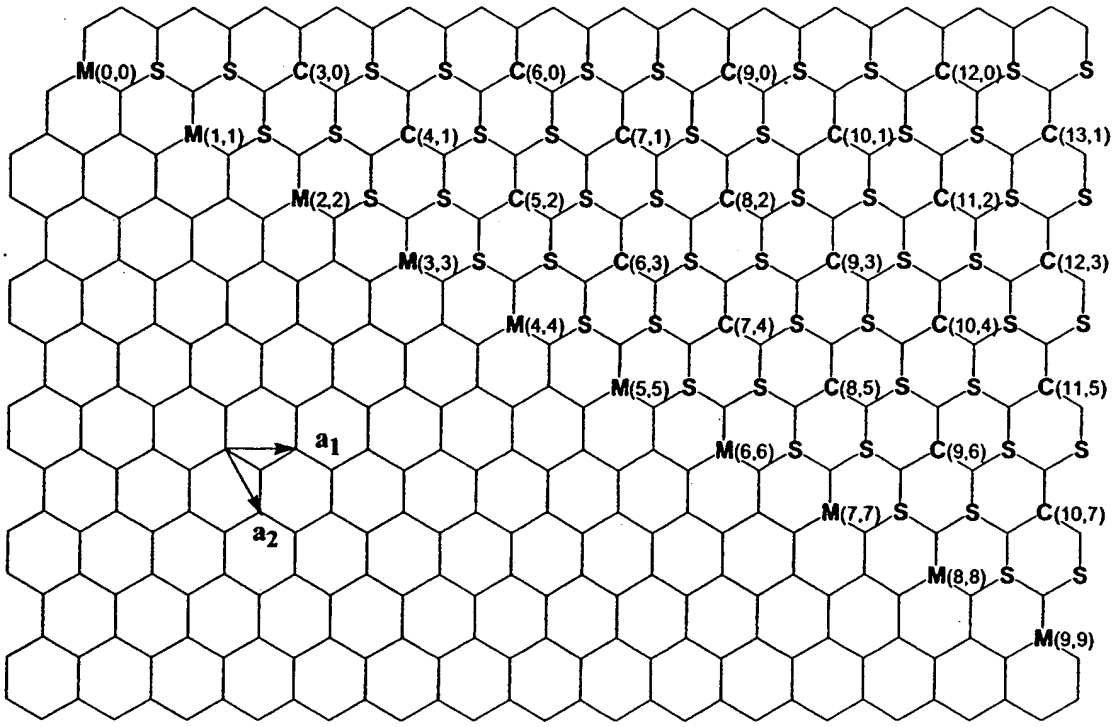

Figure 4. A map of chiral vectors that determine the chirality of SWNTs. Each vector is specified by the (*n*,*m*) indices. M, S, and C denote metals, semiconductors, and curvature induced small gap semiconducting SWNTs, respectively.

Table 1: Expected percentage of semiconductors, small band gap semiconductors, and metals for SWNTs with 1−3 nm diameters with no preference in chirality

	0−1 nm	1−2 nm	2−3 nm
S-SWNT	36 (62.1%)	100 (65.4%)	164 (65.6%)
SGS-SWNT	15 (25.9%)	46 (30.1%)	79 (31.6%)
M-SWNT	7 (12.1%)	7 (4.6%)	7 (2.8%)
total	58	153	250

Table 2: Experimentally revealed percentage of semiconductors, small band gap semiconductors, and metals for SWNTs (diameter = 1−3 nm) grown by CVD on ferritin-derived catalyst

	number of samples	percentage
S-SWNTs	25	62.5%
SGS-SWNTs	14	35.0%
M-SWNTs	1	2.5%
total	40	100.0%

semiconductors (S-SWNT) exhibiting characteristic conductance depletion by positive gate at room temperature (Figure 5a). Fourteen nanotubes (35%) exhibit a dip in the $I-V_g$ curve at room temperature, and the dip becomes a clear gap at low temperatures (Figure 5b). Such behavior has been observed previously and is attributed to small band gap (~10 meV) SWNTs.[22] Theoretically, the small band gaps arise for (*m*,*n*) tubes with $m-n = 3\times integer$ due to $\sigma-\pi$ orbital hybridization as a result of the nonflat nature of nanotube sidewalls.[18−21] The dip in $I-V_g$ at room temperature evolves into a depleted gap region at low temperature due to quenching of thermally excited charge carriers.[22] Only 1 out of the 40 SWNTs is assigned to an armchair metal tube showing weak gate dependence at room temperature and no conductance depletion region in the $I-V_g$ curve at low temperatures. Thus, the experimental survey reveals ~60−70% of S-SWNTs, 35% of SGS-SWNTs, and 2.5% of M-SWNTs (Table 2).

It is therefore concluded that our CVD growth conditions in fact produce SWNTs with no preference in chirality (Table 1). This result is not surprising considering the high growth temperature that can smear out the differences in thermodynamic energetics and kinetics for the growth of various chirality nanotubes. The initial nanotube nucleation process appears to be a determining step for tube chirality, after which the same chirality tends to be retained during nanotube lengthening in the base growth[1,2] mode. An important task then is to elucidate how various factors during nucleation determine the nanotube chirality by experiments and theory. These factors include growth temperature and structures of the nanoparticle seeds (diameter, shape, etc.). The interfacial structure between the nanoparticle and its supporting substrate could also play an important role. Understanding and controlling these factors will be indispensable to controlling nanotube chirality.

For device fabrication with CVD tubes, we have found large numbers of individual SWNTs that are FET-like semiconductors. The yield of metallic SWNT devices is quite low. Contrary to the CVD case, when experimenting with laser ablation[23] SWNTs, we observe a much higher percentage of nondepletable metallic SWNTs. Laser ablation does favor the growth of armchair tubes, a result that has been suggested by diffraction[23,24] measurements. Despite the lack of selectivity in chirality, the near 70% "natural abundance" of semiconductors in CVD SWNTs is welcome and places

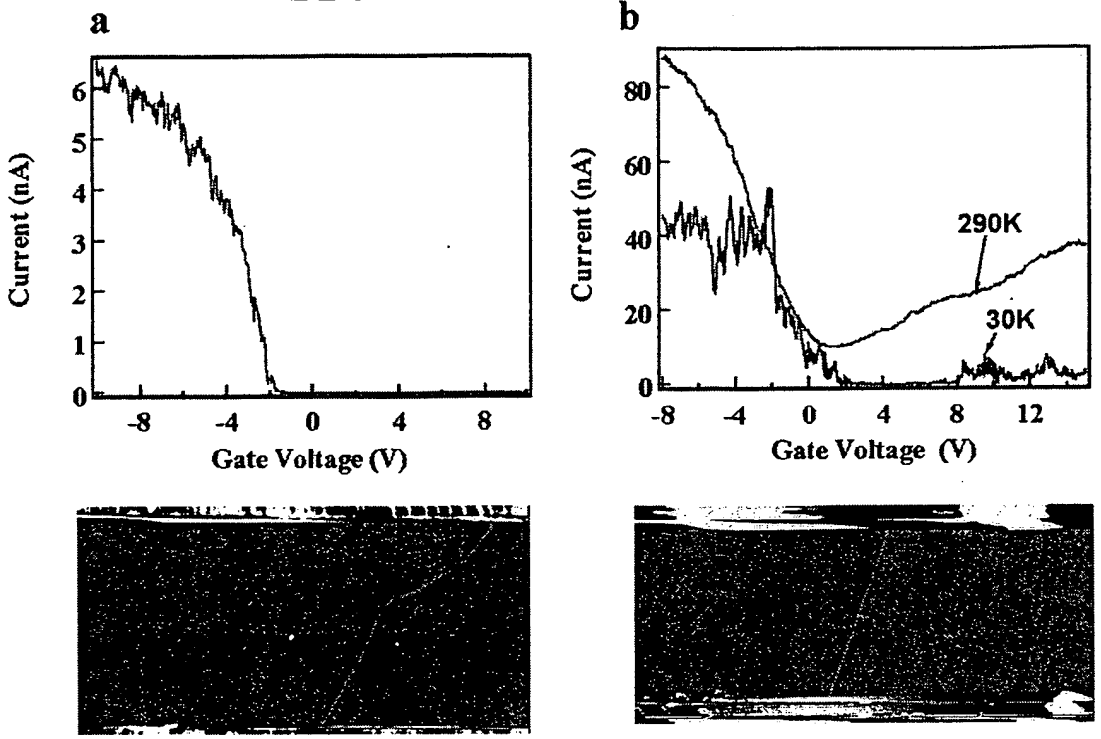

Figure 5. Representative $I-V_g$ curves recorded with (a) semiconducting SWNTs and (b) small band gap semiconducting SWNTs. Bias = 10 mV. The AFM images below the curves correspond to the single-nanotube devices. Top and bottom regions of the images are the edges of metal electrodes.

CVD nanotubes over laser materials for building transistors and sensors,[25-27] to which semiconductors are imperative. With patterned CVD growth, we are able to obtain small arrays of nanotube FETs in 100 × 100 μm^2 areas with ease. The yield for building such arrays with CVD approach is much higher than that obtainable with the approach of processing laser ablation SWNTs. Results of functional electronics and sensor arrays built with multiple-tube FETs will be presented in a future communication. We also note a useful application of the very long semiconducting SWNTs: they can be exploited for building large numbers of *identical* FETs and sensors along their lengths.

In summary, we have reported CVD synthesis of very long single-walled carbon nanotubes from well-defined catalyst nanoparticles patterned on SiO_2 substrates. The growth rate of SWNTs is found to be >60 μm/min. The long and slender SWNTs tend to form loops and closed rings along the lengths due to favorable van der Waals interactions between tube walls and high thermal energy at the growth temperature. These morphologies could be useful for exploring mesoscopic physics in quasi-1D ring structures. On the other hand, for certain applications, the ability of applying forces to nanotubes by electric fields during CVD[28] growth should allow the loop and ring formation to be manipulated or eliminated. Further, we have revealed that the CVD method produces high yield of semiconducting SWNTs. The natural abundance of semiconductors can already be exploited for building arrays of field effect transistors and sensors. We are currently exploring growth conditions that may shift the chirality distribution toward more semiconductors or metals. The task is daunting but worthwhile.

Acknowledgment. We thank useful discussions with Profs. C. Quate, J. Brauman, C. Chidsey, and N. Franklin. This work is supported by the MARCO MSD Focus Center, the Packard Foundation, the Sloan Foundation, a Terman Fellowship, and a Camile Dreyfus Teacher–Scholar Fellowship.

References

(1) Li, Y.; Kim, W.; Zhang, Y.; Rolandi, M.; Wang, D.; Dai, H. *J. Phys. Chem. B* **2001**, *105*, 11424–11431.
(2) Zhang, Y.; Li, Y.; Kim, W.; Wang, D.; Dai, H. *Appl. Phys. A* **2002**, *74*, 325–328.
(3) Cheung, C.; Kurtz, A.; Park, H.; Lieber, C. *J. Phys. Chem.* **2002**, *106*, 2429–2433.
(4) Dresselhaus, M. S.; Dresselhaus, G.; Eklund, P. C. *Science of Fullerenes and Carbon Nanotubes*; Academic Press: San Diego, 1996.
(5) Dai, H. *Surf. Sci.* **2002**, *500*, 218–241.
(6) Dai, H. In *Carbon Nanotubes*; Dresselhaus, M. S., Dresselhaus, G., Avouris, P., Eds.; Springer: Berlin, 2001; Vol. 80, pp 29–53.
(7) Choi, H.; Dai, H. *manuscript in preparation* **2002**.
(8) Kong, J.; Soh, H.; Cassell, A.; Quate, C. F.; Dai, H. *Nature* **1998**, *395*, 878.
(9) Soh, H.; Quate, C.; Morpurgo, A.; Marcus, C.; Kong, J.; Dai, H. *Appl. Phys. Lett.* **1999**, *75*, 627–629.
(10) Liu, J.; Dai, H. J.; Hafner, J. H.; Colbert, D. T.; Smalley, R. E.; Tans, S. J.; Dekker, C. *Nature* **1997**, *385*, 780–781.
(11) Martel, R.; HR, H. R. S.; P, P. A. *Nature* **1999**, *398*, 299.
(12) Sano, M.; Kamino, A.; Okamura, J.; Shinkai, S. *Science* **2001**, *293*, 1299–1301.
(13) Franklin, N. R.; Li, Y.; Chen, R. J.; Javey, A.; Dai, H. *Appl. Phys. Lett.* **2001**, *79*, 4571–4573.
(14) Franklin, N.; Dai, H. *Adv. Mater.* **2000**, *12*, 890.
(15) Tans, S.; Verschueren, A.; Dekker, C. *Nature* **1998**, *393*, 49–52.
(16) Chen, R.; Franklin, N.; Kong, J.; Cao, J.; Tombler, T.; Zhang, Y.; Dai, H. *Appl. Phys. Lett.* **2001**, *79*, 6951.
(17) Saito, R.; Fujita, M.; Dresselhaus, G.; Dresselhaus, M. S. *Appl. Phys. Lett.* **1992**, *60*, 2204.

(18) Hamada, N.; Sawada, S.-i.; Oshiyama, A. *Phys. Rev. Lett.* **1992**, *68*, 1579−1581.
(19) White, C. T.; Robertson, D. H.; Mintmire, J. W. In *Clusters and Nanostructured Materials*; Jena, P., Behera, S., Eds.; Nova: New York, 1996; p 231.
(20) Blase, X.; Benedict, L. X.; Shirley, E. L.; Louie, S. G. *Phys. Rev. Lett.* **1994**, *72*, 1878−1881.
(21) Kane, C. L.; Mele, E. J. *Phys. Rev. Lett.* **1997**, *78*, 1932−1935.
(22) Zhou, C.; Kong, J.; Dai, H. *Phys. Rev. Lett.* **2000**, *84*, 5604.
(23) Thess, A.; Lee, R.; Nikolaev, P.; Dai, H. J.; Petit, P.; Robert, J.; Xu, C. H.; Lee, Y. H.; Kim, S. G.; Rinzler, A. G.; Colbert, D. T.; Scuseria, G. E.; Tomanek, D.; Fischer, J. E.; Smalley, R. E. *Science* **1996**, *273*, 483−487.
(24) Cowley, J.; Nikolaev, P.; Thess, A.; Smalley, R. *Chem. Phys. Lett.* **1997**, *265*, 379−384.
(25) Kong, J.; Franklin, N.; Zhou, C.; Chapline, M.; Peng, S.; Cho, K.; Dai, H. *Science* **2000**, *287*, 622−625.
(26) Kong, J.; Chapline, M.; Dai, H. *Adv. Mater.* **2001**, *13*, 1384−1386.
(27) Kong, J.; Dai, H. *J. Phys. Chem.* **2001**, *105*, 2890−2893.
(28) Zhang, Y.; Chan, A.; Cao, J.; Wang, Q.; Kim, W.; Li, Y.; Morris, N.; Yenilmez, E.; Kong, J.; Dai, H. *Appl. Phys. Lett.* **2001**, *79*, 3155−3157.

NL025602Q